

Cross slide mathematical model for solving chatter

Jiří Ondrášek

VÚTS, a.s./Mechatronics Department, Svárovská 619, 460 01 Liberec XI, Czech Republic,
e-mail: jiri.ondrasek@vuts.cz

Abstract—The paper deals with the issues of creating a mathematical model of self-excited chatter of the cross slide. This type of oscillation occurs in systems where there is still an internal source from which the system consumes energy to maintain or even to increase the amplitude of oscillation. This consumption is controlled by an oscillatory movement of the system itself. Such an energy source greatly affects the dynamic and stability properties of the system.

Keywords—chatter, cross slide, chip thickness, lobe diagram

I. INTRODUCTION

One of the main causes of generating self-excited vibration in mechanical systems is dry friction between two mutually moving parts that are directly related to damping in the system. Chatter is undesirable and there are efforts to avoid it either by increasing positive damping or eliminating the causes of negative damping. The frequency of steady chatter is close to the natural frequency of a mechanical system.

This phenomenon often occurs during machining operation when a part of the energy of cutting process during cutting operation can change in the energy oscillating the machine as a whole. Vibration then manifests in a significant waviness of the cut surface and is usually accompanied by noise. Generally, it is theoretically possible to establish a certain range of cutting conditions under which, when applying them, no chatter arises. One of the means of such a designation is speed stability diagram – *lobe diagram*, which expresses the dependence of chip thickness on the workpiece speed. The methodology of creating lobe diagrams is based on the Laplace transform images of the cutting force and movement of a tool group in the direction of material removal.

The very issue of dealing with chatter in cutting machining operation is creating the mathematical models of the following physical objects: *Model of the machining process*, *Model of mechanical system inclusive flexible links and real constraints*, *Drive model that presents a model of electromotor itself and its control*.

II. CHATTER

A mathematical process of machining process is described in detail in publication [2], see Chapter 5, a brief description of continuous machining is given in article [1], as the case may be. In the case of creating a mathematical model of the cross slide to investigate chatter it is assumed the latter mentioned method of machining. For this reason and for the reason of the logical linking of mathematical models of particular

objects, in the following part of the text there are again provided some basic relationships of continuous cutting machining operation that are based on those assumptions:

1) Cutting force F is proportional to width b and depth of cut y_N in the direction of the normal to the machined surface by the relation:

$$F = -C_0 b y_N. \quad (1)$$

2) Cutting force constant C_0 is independent of speed.

3) Cutting edge geometry does not affect the direct correlation between force F and chip depth y_N in the normal direction.

4) Angle β (an angle between cutting force F and the axis perpendicular to the normal of the machined surface) does not change with chip depth y_N .

5) Friction forces between tool, workpiece and leaving chip are neglected.

In **Fig. 1**, there is shown a block diagram of the continuous machining process in which the dynamic system can be described by the so-called oriented dynamic compliance $G_y(s)$. This is a transfer function between the Laplace transforms of cutting force $F(s)$ and the movement of the tool group $y(s)$:

$$G_y(s) = \frac{y(s)}{F(s)}, \quad (2)$$

where s is the complex variable.

If depth of chip $y_0(t) < 0$ is specified, cutting force F is generated which will cause the movement of tool group $y(t)$ that will be superimposed to the specified depth, so instantaneous chip depth $y_N(t)$ is given by an expression:

$$y_N(t) = y_0(t) + y(t). \quad (3)$$

The chip thickness is negative because chip cutting occurs in the opposite direction of the y -axis orientation. If there is a case of $y_N(t) > 0$, the cutting edge got out from engagement. When working with a fixed time link between the cuts, the freshly machined surface will get again into contact with the tool after a defined time with the so-called transport time delay T_d . This fact can be expressed with a relation:

$$y_N(t) = y_0(t) + y(t) - y(t - T_d), \quad (4)$$

where $y_0(t)$ is the feed per one revolution, term $y(t)$ is valid for immediate waviness and term $y(t - T_d)$ applies for waviness from the previous cut which will come under the cutting edge of the tool over a time period T_d .

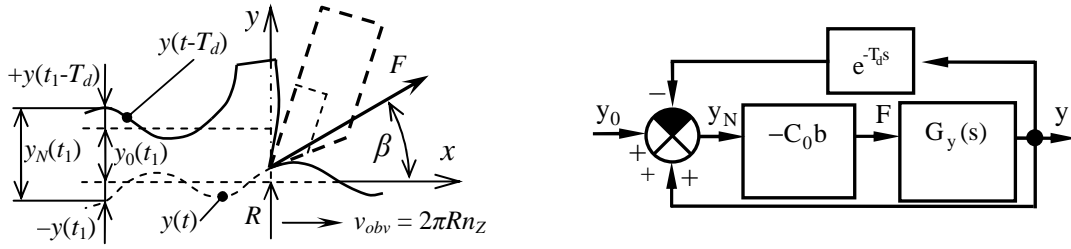


Fig. 1. Continuous machining and its block diagram.

Waviness $y(t-T_d)$ from the previous cut together with an immediate tool position $y(t)$ always affects the variation of chip depth $y_N(t)$, see **Fig. 1**, where the instantaneous chip depth y_N at time $t = t_1$ is shown. The Laplace image of equation (4) is:

$$y_N(s) = y_0(s) + y(s)(1 - e^{-T_d s}). \quad (5)$$

Using equations (1), (2) and (5), the closed loop transfer as to **Fig. 1** can be determined in the following form:

$$G_{\text{celk}}(s) = \frac{y(s)}{y_0(s)} = \frac{-C_0 b G_y(s)}{1 + C_0 b G_y(s)(1 - e^{-T_d s})}. \quad (6)$$

To ensure the stability of the machining process it is necessary so that chip width b does not exceed the limit chip width b_{mez} at which the amplitude characteristic of the closed loop transfer (6) shall not exceed the unit level at any angular frequency ω . This condition is expressed by the relationship:

$$b < b_{mez} = -\frac{1}{2C_0 (\text{Re}_{neg} G_y(j\omega))_{\min}} = \text{funkcel}(\omega), \quad (7)$$

in which $\text{Re}_{neg} G_y$ represents negative values of the real component of dynamic compliance G_y , see [2].

The stability lobe diagram expresses the dependence of limit chip width b_{mez} on the speed of workpiece n_Z . The speed equation, see [1], is given by the expression:

$$f = n_Z \left(N + 1 - \frac{1}{\pi} \arctg \frac{\text{Re} G_y(j\omega)}{\text{Im} G_y(j\omega)} \right) = \text{funkce2}(\omega), \quad (8)$$

where $f = \omega/2\pi$ is the frequency of self-excited vibrations on the limit of stability for each value of N individually. Number N indicates the number of whole waves of the workpiece surface ripple to be incurred over period $T_d = 1/n_Z$. The full version of the stability lobe diagram is generated in practice as follows:

1) To the theoretically or experimentally determined set of the values of dynamic compliance, there are completed arranged pairs $f \leftrightarrow b_{mez}$ as to (7).

2) By means of (8), there are created pairs $f \leftrightarrow n_Z$ repeatedly for values $N = 0, 1, 2, \dots$ which may be further displayed by a set of curves $f = f(n_Z)$.

3) From pairs $f \leftrightarrow n_Z$ and $f \leftrightarrow b_{mez}$, there are assembled pairs $n_Z \leftrightarrow b_{mez}$ which are shown as a set of curves – *lobs* for various values N again.

4) The individual „*lobs*“ may intersect each other and the area of the stable widths is under their lower envelope.

III. EFFECT OF FEED DRIVES ON THE CHATTER

The shape of speed diagram and defining the areas of stability in the diagram depend, in addition to the properties of the coupled mechanical system, also on the characteristics of feed drives. In the same way as the behavior and properties of a mechanical system, also the behavior and properties of a control drive can be considered. They are commonly expressed by the dynamic flexibility of the control when it is again a transfer function. The total dynamic compliance of the associated dynamic system is then determined on the basis of the causal interconnection of particular dynamic systems, i.e., feed drives and a mechanical system. This interconnection is simple since the outputs of the one system are inputs of the second system, as shown in **Fig. 2** and **Fig. 3**.

In computer simulations it is assumed that the drive of the feeds of machine tool will be implemented by a 3phase synchronous electromotor with permanent magnets with which an exciting magnetic rotor flow is produced. For the purposes of simulations, the model of this servomotor was replaced by a simplified model which is based on the description of a DC motor, see **Fig. 2**, in which the block *Mechanical system* is a motor rotor with mass moment of inertia J . The parameters of a single coil, i.e., inductance L_s , electrical resistance R_s and motor voltage constant K_E are substituted in this model. Only at torque constant K_T it is necessary to substitute the value:

$$K_{T\text{celk}} = \frac{3}{2} K_T, \quad (9)$$

whereby the common interaction of all three coils is taken into account, see [4]. Furthermore, in the scheme, there stands U for voltage, I electrical current, M electromagnetic torque, ω rotor angular velocity and φ rotor angular displacement. The above given parameters of the electromotor were substituted in its simulation model from the data sheet stated by the manufacturer.

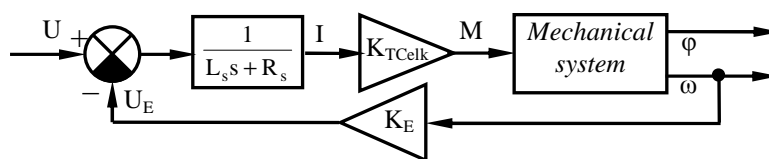


Fig. 2. A simplified block diagram of a synchronous motor.

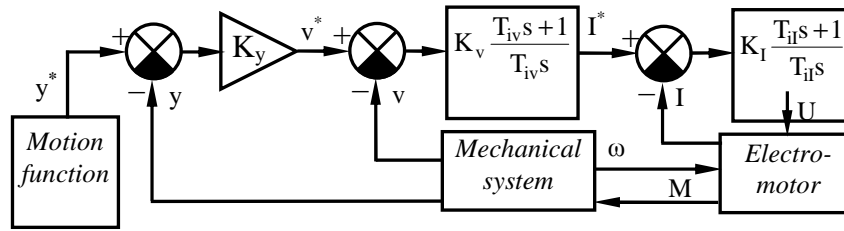


Fig. 3. A cascade control circuit with a current speed and position feedback.

In the vector control of this type of electric motor, it is almost exclusively used the cascade control circuit with three hierarchically arranged feedbacks: current, speed and position, see Fig. 3. Maintaining the required values of position, revolutions and current is ensured by PID linear controllers. Constant K is a proportional component of the controller, constant T_i expresses the integral time constant of the controller and T_d is a derivative time constant, $v = y, \dot{y}, I$. Index v reflects competence of the various constants to the position, velocity and current feedback. Those constants in the control structure according to Fig. 3 were debugged for the needs of the simulation model by the Ziegler-Nichols method, see [5]. In the diagram in Fig. 3, y expresses the position of the tool group, v its velocity, and $*$ denotes the desired value of a particular variable.

IV. MATHEMATICAL MODEL OF A MECHANICAL SYSTEM

A. Mathematical description of a coupled mech. system

To build equations of motion of a coupled mechanical system with flexible links, it is usually based on the Lagrange equations of mixed type which in matrix form are as follows:

$$\frac{d}{dt} \left(\frac{\partial E_k}{\partial \dot{\mathbf{q}}} \right) - \left(\frac{\partial E_k}{\partial \mathbf{q}} \right) + \left(\frac{\partial E_p}{\partial \mathbf{q}} \right) + \left(\frac{\partial R_d}{\partial \dot{\mathbf{q}}} \right) = \mathbf{Q} + \left[\frac{\partial \mathbf{f}^V}{\partial \mathbf{q}} \right] \boldsymbol{\lambda}, \quad (10)$$

where E_k and E_p represent the kinetic and potential energy of a mechanical system, R_d the so-called Rayleigh dissipative function and vector \mathbf{Q} represents the vector of action generalized forces whose components correspond to appropriate coordinates q_j . To describe the coupled mechanical system, there are used generally dependent physical coordinates \mathbf{q} of dimension r , which are coupled by a system s of scalar constraint conditions:

$$\mathbf{f}^V(\mathbf{q}, t) = \mathbf{0}. \quad (11)$$

For i -th flexible (pliable) body, coordinate vector \mathbf{q}_i can be written as:

$$\mathbf{q}_i = [\mathbf{r}_i, \mathbf{p}_i, \mathbf{q}_{ei}],$$

in which \mathbf{r}_i is the vector of the coordinates that define the location of the given body in a fixed coordinate system $Oxyz$. Orientation of the body in the basic space is determined with Euler parameters \mathbf{p}_i . The elastic deformations of the body are expressed by the vector of elastic (or standardized modal) coordinates \mathbf{q}_{ei} . Furthermore, in equations (10), vector $\boldsymbol{\lambda}$ of Lagrange multipliers is found in the number of s that have a direct connection with the reactionary forces in kinematic constraints. The coupled mechanical system is characterized by $i = r - s$ degrees of freedom.

Knowing kinetic E_k , potential E_p , and dissipative R_d energies of the coupled mechanical system, it is possible to establish equations of motion. Together with the second time derivative of constraint conditions \mathbf{f}^V , a summary record of these equations in matrix form can be included:

$$\begin{bmatrix} \mathbf{M} & -\mathbf{J}^T \\ \mathbf{J} & \mathbf{0} \end{bmatrix} \begin{bmatrix} \ddot{\mathbf{q}} \\ \boldsymbol{\lambda} \end{bmatrix} = \begin{bmatrix} \mathbf{p}_1 - \mathbf{D}\dot{\mathbf{q}} - \mathbf{K}\mathbf{q} \\ \mathbf{p}_2 \end{bmatrix}. \quad (12)$$

in which:

$$\mathbf{J} = \frac{\partial \mathbf{f}^V}{\partial \mathbf{q}^T} \quad (13)$$

expresses the Jacobi matrix of the system of coupling equations. Symbols \mathbf{M} , \mathbf{K} and \mathbf{D} are gradually mass, stiffness and damping matrices of the mechanical system as a whole. Vectors \mathbf{p}_1 and \mathbf{p}_2 are:

$$\begin{aligned} \mathbf{p}_1 &= \mathbf{Q} - \mathbf{f}^g - \dot{\mathbf{M}}\dot{\mathbf{q}} + \frac{1}{2} \left[\frac{\partial \mathbf{M}}{\partial \mathbf{q}} \dot{\mathbf{q}} \right]^T \dot{\mathbf{q}}, \\ \mathbf{p}_2 &= -\frac{\partial}{\partial \mathbf{q}^T} (\mathbf{J}\dot{\mathbf{q}}) - 2 \frac{\partial}{\partial \mathbf{q}^T} \left(\frac{\partial \mathbf{f}^V}{\partial t} \right) \dot{\mathbf{q}} - \frac{\partial^2 \mathbf{f}^V}{\partial t^2}, \end{aligned} \quad (14)$$

where vector \mathbf{f}^g is the vector of gravitational forces.

Equations (12) compose a system $(r+s)$ of algebraic-differential equations for r unknown generally dependent physical equations \mathbf{q} and s unknown Lagrange multipliers $\boldsymbol{\lambda}$. These equations are currently assembled and solved by *computational mechanics*.

Comprehensive information about creating mathematical models of multibody systems with flexible bodies is cited e.g. in publication [3].

B. Frequency response of the coupled mechanical system

Transfer functions between the acting forces and the mass displacements of the controlled mechanical system with discretely distributed mass and stiffness parameters are generally determined by the relevant matrix elements:

$$\mathbf{G}(s) = (\mathbf{M}s^2 + \mathbf{D}s + \mathbf{K})^{-1}. \quad (15)$$

The method of determining the transfer function of the mechanical system according to relation (15) is applicable only for linear non-conservative mechanical systems. In the case of mechanical systems in which there occur nonlinearities due to passive resistances in kinematic constraints for example, it is advisable to use a method in which the system is excited by the swept signal. It is one of the possible methods that allows the study of nonlinearities in the time domain only. Getting a frequency response of a nonlinear dynamic system is possible only round about the operating point.

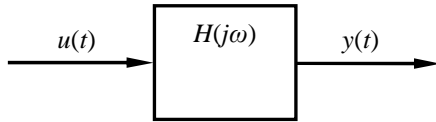


Fig. 4. Time-invariant system block.

Consider a dynamic system described by the frequency response:

$$H(j\omega) = \frac{Y(j\omega)}{U(j\omega)}, \quad (16)$$

where $Y(j\omega)$ and $U(j\omega)$ are the images of output and input signal $y(t)$ and $y(t)$, see **Fig. 4**. Because it is a complex function, it can be decomposed into the real and imaginary parts:

$$H(j\omega) = V(\omega) + jW(\omega), \quad (17)$$

with which the amplitude part $A(\omega)$ and the phase part $\varphi(\omega)$ of frequency response can be determined:

$$\begin{aligned} A(\omega) &= |H(j\omega)| = \sqrt{V^2(\omega) + W^2(\omega)}, \\ \varphi(\omega) &= \arg(H(j\omega)) = \arctan\left(\frac{W(\omega)}{V(\omega)}\right). \end{aligned} \quad (18)$$

Alternatively:

$$\begin{aligned} \operatorname{Re}\{H(j\omega)\} &= |H(j\omega)| \cos \varphi(\omega), \\ \operatorname{Im}\{H(j\omega)\} &= |H(j\omega)| \sin \varphi(\omega). \end{aligned} \quad (19)$$

If a swept sine wave signal is fed to the system input:

$$u(t) = A_1 \sin(\pi f_0 t^2), \quad (20)$$

then, a signal with variable frequency and amplitude will be stabilized at the system output:

$$y(t) = A_2(t) \sin(\omega(t)t + \varphi_0). \quad (21)$$

Subsequently, both signals are converted with Fourier transformation into the frequency domain and by their dividing according to (16), it is set the appropriate frequency response around the given operating point. In other words, there is a linear approximation of the appropriate transfer function.

C. The natural frequency of the coupled mech. system

If the coupled mechanical system is generally expressed in a system of equations of motion in matrix form:

$$\mathbf{M}\ddot{\mathbf{q}}(t) + \mathbf{D}\dot{\mathbf{q}}(t) + \mathbf{K}\mathbf{q}(t) = \mathbf{f}(t), \quad (22)$$

it can be solved at $\mathbf{f}(t) = \mathbf{0}$ the problem of eigenvalues, which is given in n -dimensional space by the expression:

$$\det(\lambda^2 \mathbf{M} + \lambda \mathbf{D} + \mathbf{K}) = 0. \quad (23)$$

Roots λ_i of the characteristic equation (23) are the eigenvalues of the system. Those can be complex coupled in pairs:

$$\lambda_i = -\alpha_i + j\beta_i, \quad \lambda_i^* = -\alpha_i - j\beta_i, \quad i = 1, 2, \dots, m$$

or real:

$$\lambda_i = -\alpha_i, \quad i = 2m + 1, 2m + 2, \dots, n.$$

If any of the eigenvalues should have a positive real part, it would be an unstable mechanical system. The relationship between the imaginary part of the eigenvalue β_i and the natural frequency of the system Ω_{0i} is determined by the following conversion:

$$\Omega_{0i} = \frac{\beta_i}{2\pi}. \quad (24)$$

V. MATHEMATICAL MODEL OF A CROSS SLIDE

The aim of the calculations in the mathematical model of the chatter of the cross-slide was to calculate the limit chip width b_{mez} and to create the stability lobe diagram in the machining processes of grooving (machining in u -direction) and longitudinal turning (machining in w -direction) while both operations do not occur simultaneously. To establish them, it is necessary to determine the appropriate dynamic compliance $G_y(s)$, $y = u, w$, in the given direction depending on the method of machining.

As stated above, the problems of vibration during machining can be divided into the description of three basic objects:

- 1) The process of cutting itself.
- 2) The description of the mechanical system – machine tool or machine group.
- 3) Description of the drive, i.e., the engine itself and its control.

In the first case it was used the knowledge contained primarily in [2], and which are briefly mentioned in the previous Chapter II. Here are two parameters that, on the basis of assumptions, were considered for constants that had to be put into the resulting simulation model. These are:

- $\beta = 22.5^\circ$ cutting angle,
- $C_0 = 2 \cdot 10^9 \text{ Nm}^{-2}$ cutting force constant.

A cross slide mathematical model is generally expressed in equation (12), see **Fig. 5**. These equations were compiled based on the following assumptions.

This is a spatial system of 24 perfectly rigid bodies (without considering the frame 1) and 4 flexible bodies – a console of U and W axes and a slide of U and W axes. Between the bodies there were defined kinematic pairs in such a way so that the analyzed mechanical system is free of redundant constraints.

W axis console seating to the frame, ball screw support, ball screw nut and the ball screw itself of both axes were considered as flexible. Their compliance was defined by stiffness as to TABLE I. Stiffness of both ball screws is given by the ball screw nut distance from the ball screw support. These are the following:

$$l_U = 125 \text{ mm}, \quad l_W = 140 \text{ mm}.$$

Both ball screws are overhung.

TABLE I.
STIFFNESS OF FLEXIBLE ELEMENTS

	Unit	U -axis	W -axis
Torsion stiffness of the coupling	$[\text{Nmrad}^{-1}]$	825	825
Screw support stiffness	$10^6 [\text{Nm}^{-1}]$	450	450
Nut axial stiffness	$10^6 [\text{Nm}^{-1}]$	410	410
Screw longitudinal stiffness	$10^6 [\text{Nm}^{-1}]$	688	614
Screw torsion stiffness	$[\text{Nmrad}^{-1}]$	17620	15730

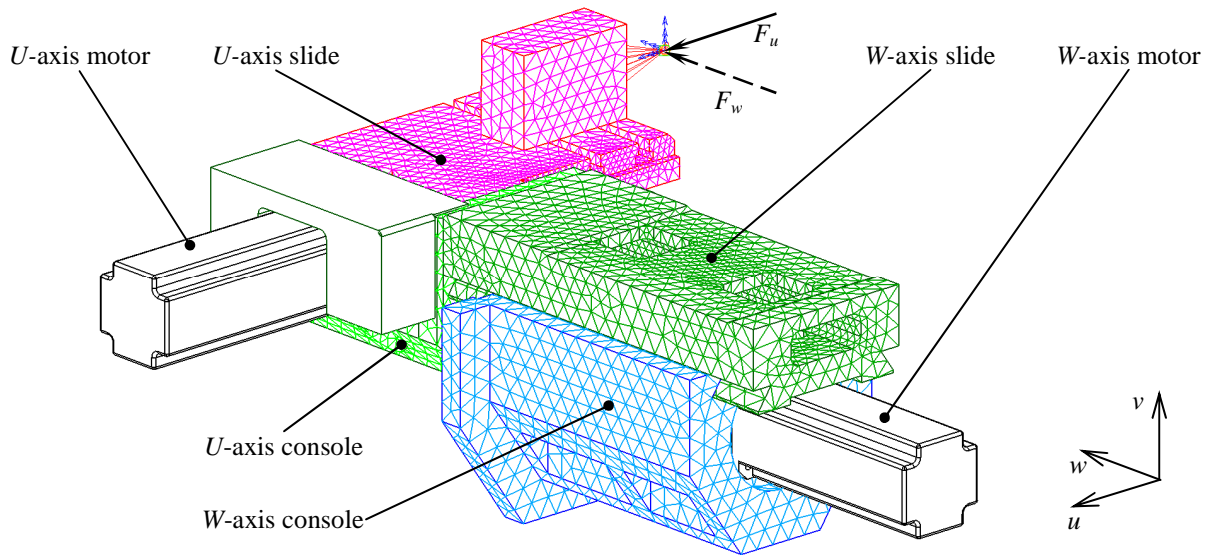


Fig. 5. Cross slide model.

The damping of these elements was selected proportional to their stiffness in the simulation model, i.e.:

$$d_{U,W} = 2.5 \cdot 10^{-6} k_{U,W}$$

in the case of longitudinal stiffness and

$$d_{tU,W} = 2.5 \cdot 10^{-3} k_{tU,W}$$

in the case of torsion stiffness.

The deformation field of the flexible bodies was approximated with deformation modes, see [3]. It is a linear combination of static wave shapes of the body that respect the boundary conditions and the natural vibrations of the given flexible body. The modes of individual elements were established on the basis of the model of the particular body, created by using the FEM. Through those modes, there were determined further generalized mass matrix **M** and stiffness matrix **K** of the given flexible body whose dimension was acceptable for the purposes of subsequent calculations already. Damping matrix **D** of the flexible body was defined on the basis of modal damping coefficients c_i . That one was introduced by means of damping ratio b_{ri} that expresses the ratio of c_i modal damping coefficient in relation to c_i^{cr} critical damping of the given mode of the appropriate pliable body. The coefficients of proportional damping and damping ratio were verified with respect to the experimentally determined modal damping of the natural wave shapes with the real mechanical system.

TABLE II.
PROPORTIONAL DAMPING OF THE OWN SHAPES OF PLIABLE BODIES

	b_{ri} [%]
W axis console	10
W axis slide + U axis console	25
U axis slide	20

The dovetail slides of the cross slide were modeled through the interaction of two bodies. It is ensured by the action of coupling forces as linear dampers with b_v damping coefficients. The origin of forces is spread over

6 points in each functional area of each from the dovetail slides of *U* and *W* machining axes. This gives a total of 2x24 force relations between two pairs of bodies. Points were distributed evenly in such a way so that the appropriate pairs of points can lie always opposite each other in the normal to the functional surfaces of the groove.

Oil viscosity was estimated at 250 mPa·s and the normal clearance on one side of the groove 10 μm, while these values correspond to the specific damping coefficient δ in a size of $5 \cdot 10^{10}$ Nsm⁻³. Then, damping coefficients b_v of one damper for each of the functional surfaces of the dovetail slide of *U* and *W* machining axes can be determined as follows:

$$b_v = \frac{1}{12} \delta l_v d_v, \quad v = Uh, Us, Wh, Ws, \quad (25)$$

in which *U* and *W* indices stand for belonging to *U* and *W* axes and *h* and *s* indices express the horizontal and inclined functional surface of the dovetail slide. Knowing length l_v and width d_v of the contact surfaces of the dovetail slide groove, damping coefficients b_v of linear dampers were determined and which are given in TABLE III.

TABLE III.
DAMPING COEFFICIENTS OF LINEAR DAMPERS

		l_v [mm]	d_v [mm]	$b_v \cdot 10^7$ [Nsm ⁻¹]
<i>U</i>	<i>h</i>	260	35.29	3.8
	<i>s</i>	260	19.03	2.1
<i>W</i>	<i>h</i>	304	40.30	5.1
	<i>s</i>	304	23.54	3.0

The resulting simulation model was characterized by 108 DOF.

In the model of feed drive, there were substituted the numerical values of the relevant parameters and which are given in TABLE IV.

TABLE IV.
DRIVE PARAMETERS

	Unit	Value
p_p – Number of pole pairs	[-]	3
R_s – Electrical resistance of one phase	[Ω]	1.5
L_s – Inductance of one phase	[mH]	13.3
K_E – Motor voltage constant	[Vrad]	0.4444
K_T – Motor torque constant	[NmA ⁻¹]	0.4054
r_I – Current controller proportional component	[VA ⁻¹]	0.8
T_I – Current controller time integration constant	[s]	0.004
r_ω – Speed controller proportional component	[Asrad ⁻¹]	0.75
T_ω – Speed controller time integration constant	[s]	0.05
r_θ – Position regulator proportional component	[s ⁻¹]	5

VI. SIMULATION RESULTS

At first, the mathematical model of the cross slide was verified on the basis of measured natural frequencies on a real machine installation. By comparing the values of calculated and measured natural frequencies, a quite good compliance between those variables is apparent, see TABLE V. Since according to the measurement the third mode dominates, this model was not further verified in terms of damping due to modal damping 1 of natural oscillation shape.

TABLE V.
NATURAL FREQUENCIES

Shape	Measured f_0 [Hz]	Measured modal damping [%]	Calculated f_0 [Hz]	Calculated modal damping [%]
1	118.0	2.8	118.6	1.4
2	157.0	2.6	160.0	2.6
3	260.0	2.6	252.0	2.6

In the next step, the mathematical model was verified with experimentally determined transfer functions of a real mechanical system. In this case, it is the course of inertances in the given direction. As an inertation it is called the transfer function between the Laplace images of cutting force and the acceleration of a tool group.

In the point of acting of cutting forces, the frequency variable course of harmonic force acts in the appropriate direction according to the following equation:

$$F_{u,v,w} = A_F \sin(\pi f_0 t^2), \quad A_F = 50N, \quad f_0 = 400Hz. \quad (26)$$

To determine inertance, it is necessary to know the progress of acceleration at the site. Then, both signals are converted through Fourier transformation into the frequency domain and with their division, the appropriate course is determined. In Fig. 6 up to Fig. 8, there is shown the course of real and imaginary components of the inertances of the cross slide provided both by measurements and calculations on a mathematical model of this mechanical system further then.

By comparing the courses of inertances determined by calculating in different directions with the measured ones, a very similar character of the dynamic properties of the mathematical model of the cross slide with a real object is obvious. For its further refinement it is necessary to better specify the submodel of damping caused mainly with passive resistances in the dovetail slide, which has a significant influence on the courses of inertances.

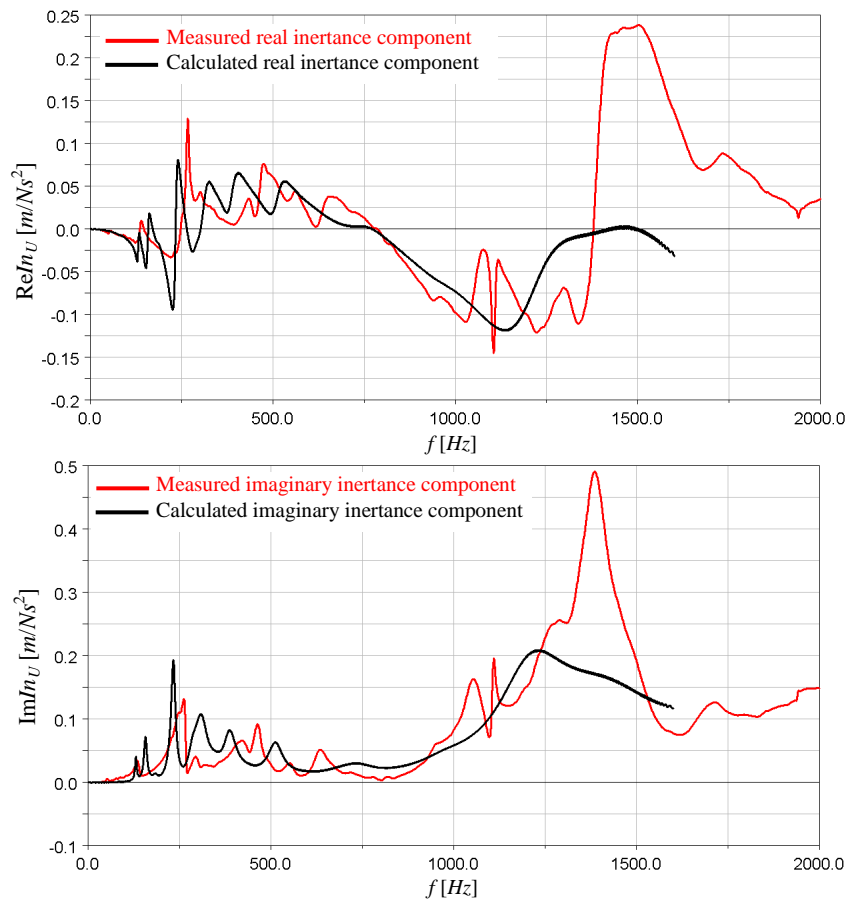


Fig. 6. Real and imaginary inertia component in u – direction.

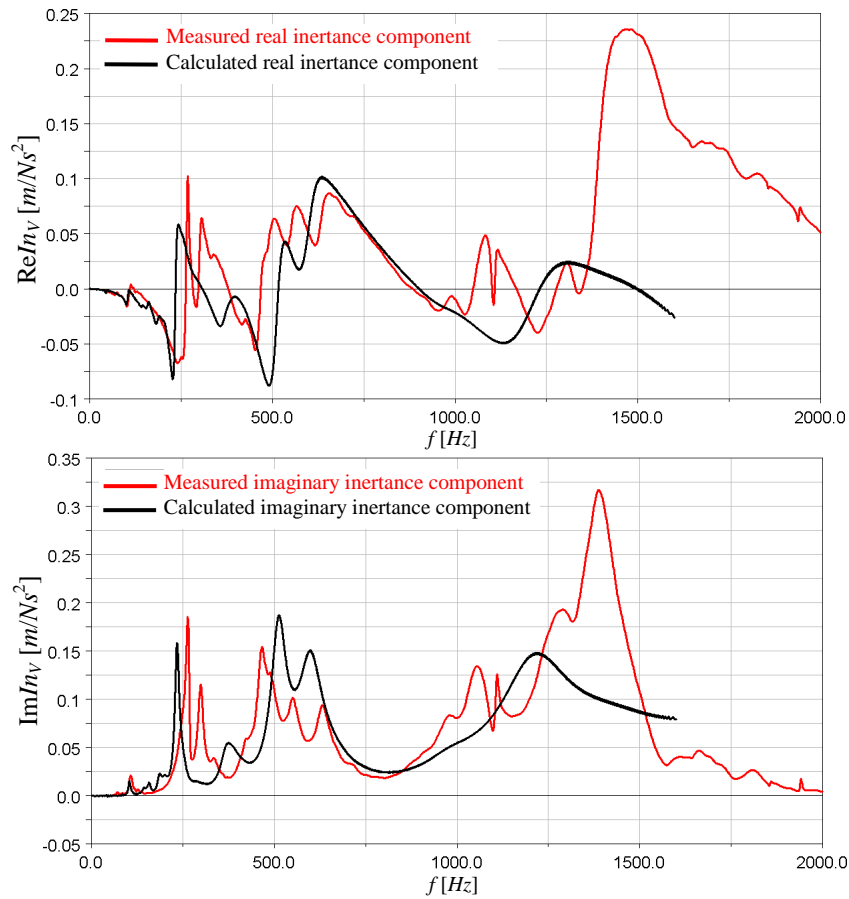


Fig. 7. Real and imaginary inertia component in v – direction.

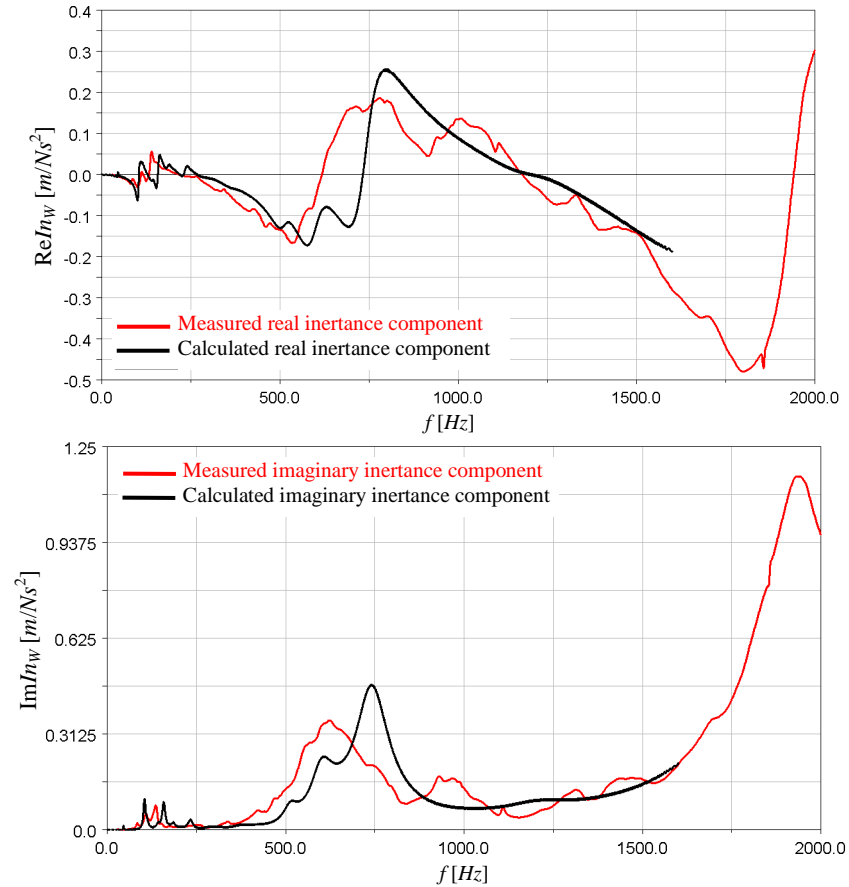


Fig. 8. Real and imaginary inertia component in w – direction.

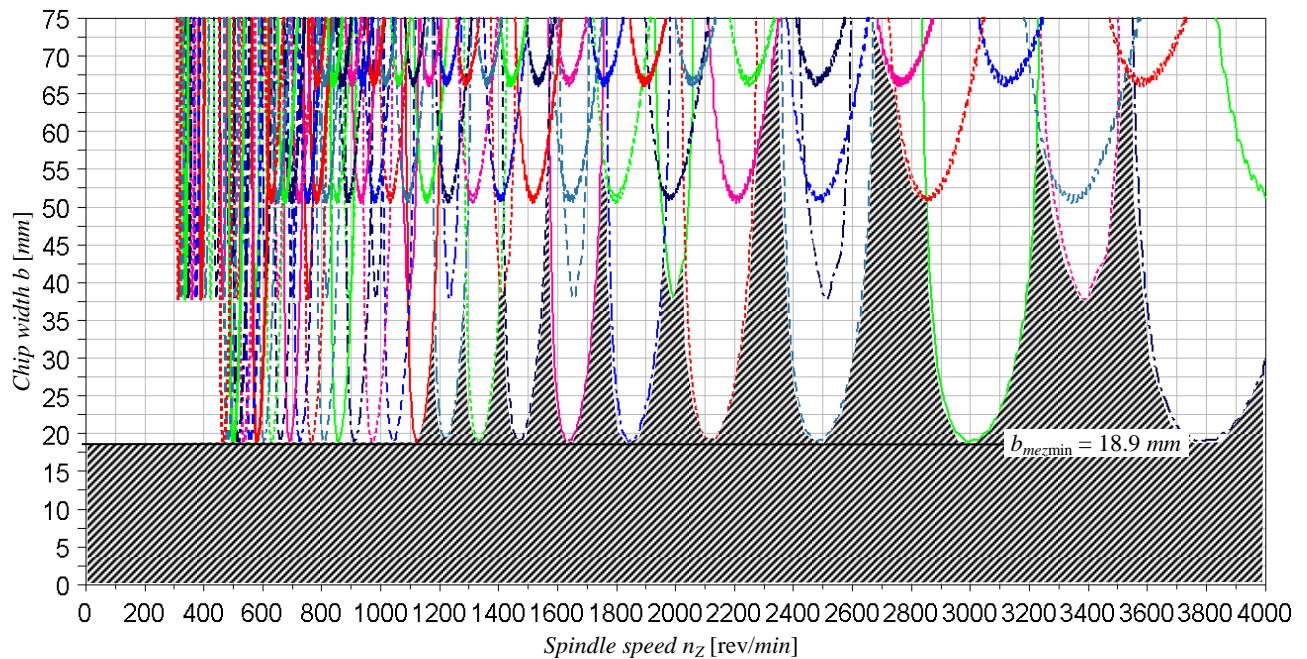


Fig. 9. Lobe diagram in the machining process of grooving.

By comparing the course of inertances determined by calculations in different directions with the measured ones, a very similar character of the dynamic features of the mathematical model of the cross slide with the real object is obvious. For its further refinement it is necessary to better specify the submodel of damping caused mainly by passive resistances in the dovetail slide that has a significant influence on the course of inertances.

A sample of the speed stability diagram of grooving is shown in Fig. 9. The diagram was designed in accordance with the procedure referred to in Paragraph II. For its formation, transfer functions determined on the basis of calculations on a mathematical model of the cross slide were used. The theoretical value of the chip minimum limit width achieves the size $b_{mezmin} = 18.9 \text{ mm}$. The stable area of cutting conditions is highlighted with hatching.

VII. CONCLUSION

Creating a mathematical model of the cross slide as a coupled mechanical system with flexible links and real constraints are not an entirely trivial matter. Especially in the case of the dynamic properties of the dovetail slide it is important to realize that this is a non-linear dynamic system. In order to take into account the dynamic properties of the real system it is necessary to create a relatively detailed computational model which leads to a large number of degrees of freedom and often shows a nonlinear character of dynamic behavior as well.

It was selected such a procedure of the creation of the linked system of the cross slide when it is a composition of abstract dynamic subsystems with causal orientation input – output. This assembly is very simple because the outputs of one model are the inputs of another model. Such a model of the related mechanical system can be solved in both time domain and frequency domain.

The course of transfer functions of the analyzed mechanical system is highly dependent on the submodel of damping - above all, on the damping in the dovetail slides of the cross slide, i.e., on passive resistances. The course of transfer functions is not significantly sensitive to the size of the specific damping coefficient δ .

The shape of Lobe diagrams depends on:

- Cutting force constant C_0 ,
- The direction of cutting force β ,
- The course of the oriented dynamic compliance of the mechanical system.

To create Lobe diagrams, it is therefore necessary to identify the internal damping of the system and the damping due to the effect of passive resistances in the given system.

ACKNOWLEDGMENT

This paper was created within the work on the 2A-2TP1/038 – Project supported by the Ministry of Industry and Trade - Ministerstvo průmyslu a obchodu.

REFERENCES

- [1] J. Ondrášek, "Creating a mathematical model for solving chatter and dealing the problems concerning the maximum allowable size of a machining chip", *Advances in Mechanisms Design, Proceedings of TMM 2012*, pp. 237-243, Springer Sciens+Business Media Dordrecht, 2012, ISBN 978-94-007-5124-8.
- [2] P. Souček, A. Bubák, *Vybrané statě z kmitání v pohonech výrobních strojů*, (in Czech), Česká technika – nakladatelství ČVUT, 2008, ISBN 978-80-01-04048-5
- [3] J. Slavík, V. Stejskal, V. Zeman, *Základy dynamiky strojů*, (in Czech), Vydavatelství ČVUT, 1997, ISBN 80-01-01622-6.
- [4] P. Souček, *Servomechanismy ve výrobních strojích*, (in Czech), Vydavatelství ČVUT, 2004, ISBN 80-01-02902-6.
- [5] M. Valášek, kolektiv, *Mechatronika*, (in Czech), Vydavatelství ČVUT, 1995, ISBN 80-01-01276-X.